

PAPER • OPEN ACCESS

Mathematical modeling of load's movement in lifter of intramill recirculation device inside tubular mill.

To cite this article: S S Latyshev *et al* 2018 *IOP Conf. Ser.: Mater. Sci. Eng.* **327** 022046

View the [article online](#) for updates and enhancements.

Related content

- [A MATHEMATICAL MODEL FOR PREDICTING NIGHT-SKY](#)
Mark A. Yocke, Henry Hogo and Don Henderson
- [DEM Investigation of Mill Speed and Lifter Face Angle on Charge Behavior in Ball Mills](#)
Zixin Yin, Yuxing Peng, Tongqing Li et al.
- [Mathematical modeling of piezoresistive elements](#)
M Geremias, R C Moreira, L A Rasia et al.



IOP | ebooks™

Bringing you innovative digital publishing with leading voices to create your essential collection of books in STEM research.

Start exploring the collection - download the first chapter of every title for free.

Mathematical modeling of load's movement in lifter of intramill recirculation device inside tubular mill.

S S Latyshev, V V Voronov, V S Bogdanov, Y M Fadin, O I Bazhanova, A N Maslovskaya

Belgorod State Technological University named after V.G. Shukhov, 46, Kostukova St., Belgorod, 308012, Russia

E-mail: Lat.sergej@gmail.com

Abstract. The paper presents the results of the mathematical modeling of load's movement in the lifter of the intramill recirculation divided inside the tubular mill. The lifter is rotating together with the mill drum and has a form of a radially mounted pipe with a hole in its side surface. The results of the mathematical modeling allowed explaining causes of load's partial sling-out from the lifter cavity and obtaining equations to describe the load's movements at different stages. The developed model allows correcting the design process of the intra-mill device and specifying the nature of its influence onto milling in the tubular mill with a higher accuracy.

1. Introduction

One of devices, used in the cement industry for fine milling of materials, is a tubular mill. Having high productivity, reliability and durability, this unit consumes an enormous amount of energy while having quite low efficiency [1 - 4].

One of disadvantages of tubular milling is prolonged presence of particles, which satisfy the requirements for the final product, in the milling area. Therefore, when milling clinker and additives, about 50% of particles meet the product fineness requirements already when they reach the end of the coarse milling chamber. These particles continue their movement along the mill barrel, not only reducing the milling intensity for large particles, but reducing the efficiency of the milling as well, by forming a very fine damping layer.

The design of an intra-mill recirculating device (**Figure 1.**) allows partially minimizing this adverse effect [5, 6]. This is achieved by organizing a recirculating flow of load inside the mill chamber. With the help of lifters 8, the load is passed to tube-auger 1, where, with the help of helical surface 2 it is transported in the reverse direction and returned into the mill chamber. Simultaneously, the flows of aspiration air strenuously act upon the material interspersed inside the tube-auger; the flows separate the small particles and move them in the direction of unloading grate 6. The sizing of the milled material in the fine mill chamber and removal of fine particles with the flows of aspiration air allows reducing time spent by the material in the mill chamber and improving the milling process efficiency [3].



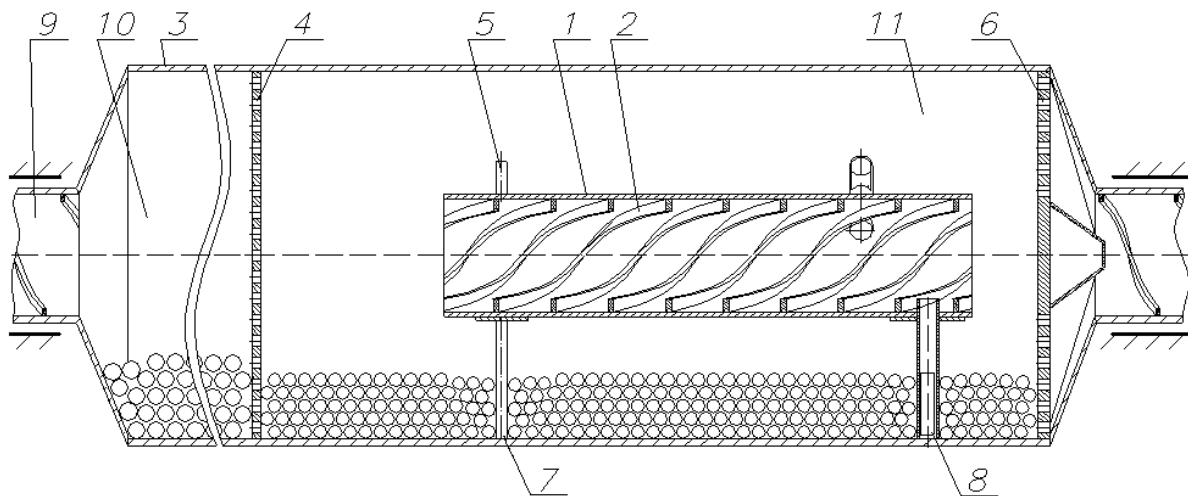


Figure 1. The intra-mill recirculation device for the tubular mill

Studies of load kinematic movements by means of high-speed photography of the grinding bodies were conducted during experimental installation to reveal specific effect that the intra-mill device has on the internal processes inside the tubular mill. The installation is a barrel mill with a transparent end. The intra-mill recirculating device is installed inside the mill's barrel.

During the experiments, a process was discovered when a part of lifter's load was returned from its cavity back to the mill chamber (**Figure 2.**); this process reduces load volume involved into the recirculation and sizing of material. Besides that, the discarded part of the lifter's load hits the barrel lining, adversely affecting its durability and that of the grinding bodies as well.



Figure 2. The results of high-speed photography of the loading movement

2. On peculiarities of load's movement in the lifter

To study the nature of load's slinging-out of the lifter's body, a mathematical modeling was performed for a point mass moving inside the lifter's cavity. The modeling was performed on the following assumptions:

- the load fills the lifter at the area, corresponding to the loading hole;
- each body of load inside the lifter's body is moving in a plane which is perpendicular to the mills' axis of rotation;
- the bodies inside the lifter's cavity move progressively with respect to the lifter's surface.

At the starting moment for the movement, along the lifter's surface (**Figure 3**), the point mass is subjected to: \vec{G} – gravity; \vec{N}_l – the force with which the lifter acts onto the body (support reaction

force);

\vec{F}_{fr} – maximum static friction force; \vec{F}_e^n – normal component of the relative force of inertia.

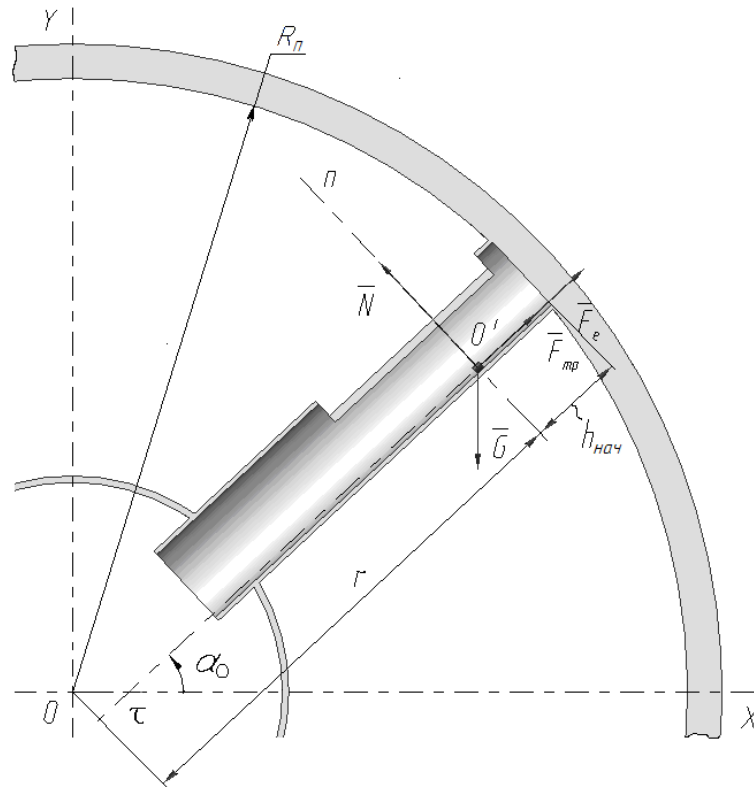


Figure 3. The starting moment of the intra-mill device's movement inside the lifter.

According to the d'Alembert's principle:

$$\vec{G} + \vec{N}_L + \vec{F}_{fr} - m\vec{a} = 0, \tag{1}$$

where m is the weight of the mass point, kg; \vec{a} is the absolute acceleration of the point mass, m/c^2 .

According to the Coriolis theorem on summation of accelerations:

$$\vec{a} = \vec{a}_r + \vec{a}_e + \vec{a}_{cor} \tag{2}$$

where \vec{a}_r is the relative acceleration of the mass point, m/s^2 ; \vec{a}_e is the translational acceleration of the mass point, m/s^2 ; \vec{a}_{cor} is the Coriolis acceleration of the mass point, m/s^2 .

The translational acceleration is represented by constant angular speed rotation, thus, \vec{a}_e is directed towards the center of rotation and its modulus is equal to:

$$a_e = \omega^2 r, \tag{3}$$

where r is the distance from the mill barrel's axis of rotation to the mass point.

$$r = R_b - h_{init}, \tag{4}$$

where R_b is the radius of the mill barrel in clear, m; h_{init} is the initial distance from the mass point to the internal surface of the barrel, m.

The relative acceleration is determined with the equation:

$$\vec{a}_r = \frac{d\vec{v}_r}{dt}, \tag{5}$$

where \vec{v}_r is the relative movement speed, m/s,

while Coriolis acceleration:

$$\vec{a}_{cor} = 2[\vec{\omega} \times \vec{v}_r]. \tag{6}$$

Thus, in the starting moment of the translational movement, $v_r = 0$:

$$\vec{a}_r = \vec{a}_{\text{cor}} = 0. \quad (7)$$

Considering equations (2), (3) and (6), equation (1) is written as:

$$\vec{G} + \vec{N}_L + \vec{F}_{\text{fr}} - m\vec{a}_e = 0. \quad (8)$$

In terms of projections onto coordinate axes $\tau_0'n$, equation (7) is written as:

$$\begin{cases} G \cdot \sin \alpha_0 - F_{\text{fr}} - ma_e = 0, \\ G \cdot \cos \alpha_0 - N_L = 0; \end{cases} \quad (9)$$

where α_0 is the angle at which the movement of the mass point along the surface of the lifter starts, in degrees.

The force of friction is determined with the equation:

$$F_{\text{fr}} = f N_L, \quad (10)$$

where f is the coefficient of sliding friction of the load on the lifter's surface.

Considering equations (3) and (9), equation (8) is written as:

$$\begin{cases} mg \cdot \sin \alpha_0 - f N_L - m\omega^2 r = 0, \\ mg \cdot \cos \alpha_0 - N_L = 0. \end{cases} \quad (11)$$

Having determined N_L from the second equation of the system (10) and inserting it into the first one, one gets:

$$mg \cdot \sin \alpha_0 - f mg \cdot \cos \alpha_0 - m\omega^2 r = 0, \quad (12)$$

Let us divide equation (11) term-by-term by the value of mg :

$$\sin \alpha_0 - f \cos \alpha_0 = \left(\frac{\omega}{\omega_0} \right)^2, \quad (13)$$

here: $\omega_0 = \sqrt{\frac{g}{r}}$; when $r = R_b$, the value of ω_0 coincides with the critical angular rotational speed of the mill barrel.

By some trivial mathematical transformations, let us transform equation (13) as:

$$\sin(\alpha_0 - \varphi_*) = \frac{\left(\frac{\omega}{\omega_0} \right)^2}{\sqrt{1+f^2}}, \quad (14)$$

where the value of friction angle φ_* is given by the equation:

$$\varphi_* = \arctg(f). \quad (15)$$

Equation (14) possesses a solution, if

$$\left(\frac{\omega}{\omega_0} \right)^2 \leq \sqrt{1+f^2}. \quad (16)$$

When friction coefficient $f = 0.3 \div 0.5$, f^2 is a small quantity in comparison with one, thus, the dependency (15) is written as:

$$\omega < \omega_0 \left(1 + \frac{1}{4} f^2 \right). \quad (17)$$

From inequality (17), it follows that equation (14) possesses a solution, if angular rotation speed ω of the mill is less than the value of $(1.0225-1.0625) \omega_0$, which holds at operating values of the angular rotational speed of the mill barrel for any distance between the mass point and the axis of rotation within the limits of the barrel's surface.

When condition (17) holds, the solution of equation (14) is written as:

$$\alpha_0 = \arctg(f) + \arcsin \frac{\left(\frac{\omega}{\omega_0} \right)^2}{\sqrt{1+f^2}} \quad (18)$$

The obtained equation allows determining an angle where the movement starts along the lifter's surface.

Radius r of the mass point inside the lifter takes values between radius R , characterizing the diameter of the mill chamber in clear, up to $R-h_{OT}$, where h_{OT} is the length of holes in the lifter. The friction coefficients takes values depending on lifter's internal surface roughness, between 0.3 and 0.5. **Figure 4** shows dependence of the starting angle of the relative movement for different mills for the friction coefficient of 0.4.

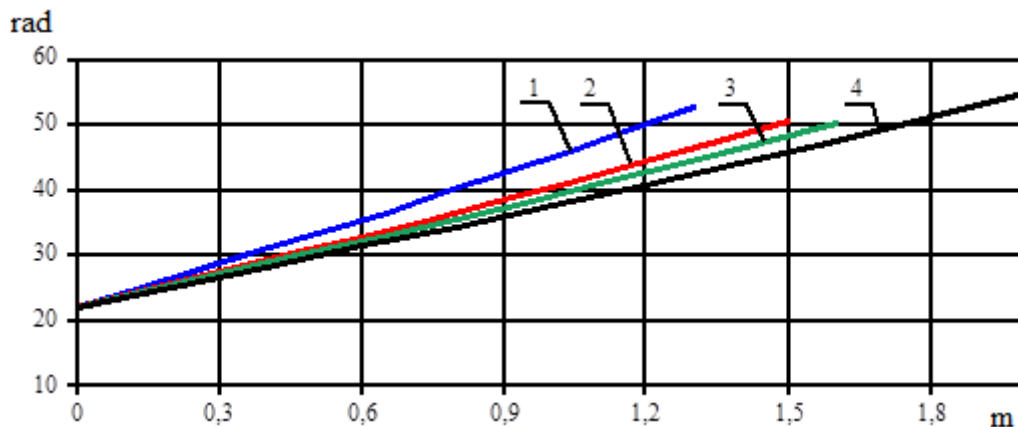


Figure 4. α_0 as a function of r when $f=0.4$ for different mills with diameters:

1 – 2.6 m 2 – 3 m; 3 – 3.2 m; 4 – 4 m.

At the first stage, the relative movement of the mass point inside the lifter's cavity proceeded in accordance with the equation:

$$m\vec{a}_r = \vec{G} + \vec{N}_L + \vec{F}_{fr} - m\vec{a}_e - m\vec{a}_{cor}, \quad (19)$$

where $m\vec{a}_e = \vec{F}_e^n$ is the relative normal force of inertia; $m\vec{a}_{cor} = \vec{F}_{cor}$ is the Coriolis force of inertia, H.

Taking into account the lack of movement along the om axis, the function describing the movement along the lifter is written like:

$$m \frac{d^2(\tau_1(t))}{dt^2} = m g \cdot \sin(\omega t) - f m g \cdot \cos(\omega t) + \quad (20)$$

$$+ 2 f m \omega \frac{d(\tau_1(t))}{dt} - m \omega^2 (R_b - h_{init} - \tau_1(t)),$$

Switching to dimensionless variables ξ and φ :

$$\xi(\varphi_R) = \frac{\tau_1(t)}{R_b}, \quad \varphi_R = \omega t, \quad (21)$$

we obtain a second-order differential equation, describing the relative movement of the mass point at the first stage:

$$\frac{d^2(\xi_1(\varphi))}{d\varphi^2} - 2f \frac{d(\xi_1(\varphi))}{d\varphi} - \xi_1(\varphi) = \left(\frac{\omega_{cr}}{\omega}\right)^2 [\sin(\varphi) - f \cos(\varphi)] - \left(1 - \frac{h_{init}}{R}\right), \quad (22)$$

whose solution shall satisfy the initial conditions:

$$\frac{d\xi_1(\alpha_0)}{d\varphi} = 0 \quad \text{and} \quad \xi_1(\alpha_0) = 0 \quad (23)$$

The second stage of the mass point movement corresponds to lifter's rotation angles $\varphi \geq \alpha_1$. Angle α_1 , reflecting the change of movement, is determined with the equation:

$$2\omega \frac{d\tau}{dt} = g \cdot \cos\alpha_1 \quad (24)$$

In this moment (the breakaway), reaction force N_{JI} of the support becomes zero, and the mass point with a certain initial speed switches to a free fall trajectory. The nature of the subsequent movement depends on the radius of the mass point's location. For load layers, which are closer to the barrel's axis than $R-h_{OT}$ during the breakaway, there is a carry-over to the opposite wall of the lifter and continuing movement along its track. For the layers which are farther than $R-h_{OT}$, there is a switch to the free fall trajectory with the further slinging out of the lifter's cavity. This is the event that was seen during the high-speed filming in the laboratory.

During the second stage, the relative movement of the mass point inside the lifter's cavity (**Figure 4.**) is described with a second-degree differential equation:

$$\frac{d^2(\xi_2(\varphi))}{d\varphi^2} + 2f \frac{d(\xi_2(\varphi))}{d\varphi} - \xi_2(\varphi) = \left(\frac{\omega_{cr}}{\omega}\right)^2 [\sin(\varphi) + f\cos(\varphi)] - \left(1 - \frac{h_{init}}{R} - \xi_1(\alpha_1)\right), \quad (25)$$

whose solution shall satisfy the initial conditions:

$$\frac{d\xi_2(\alpha_1)}{d\varphi} = \frac{d\xi_1(\alpha_1)}{d\varphi} \quad \text{and} \quad \xi_2(\alpha_1) = \xi_1(\alpha_1) \quad (26)$$

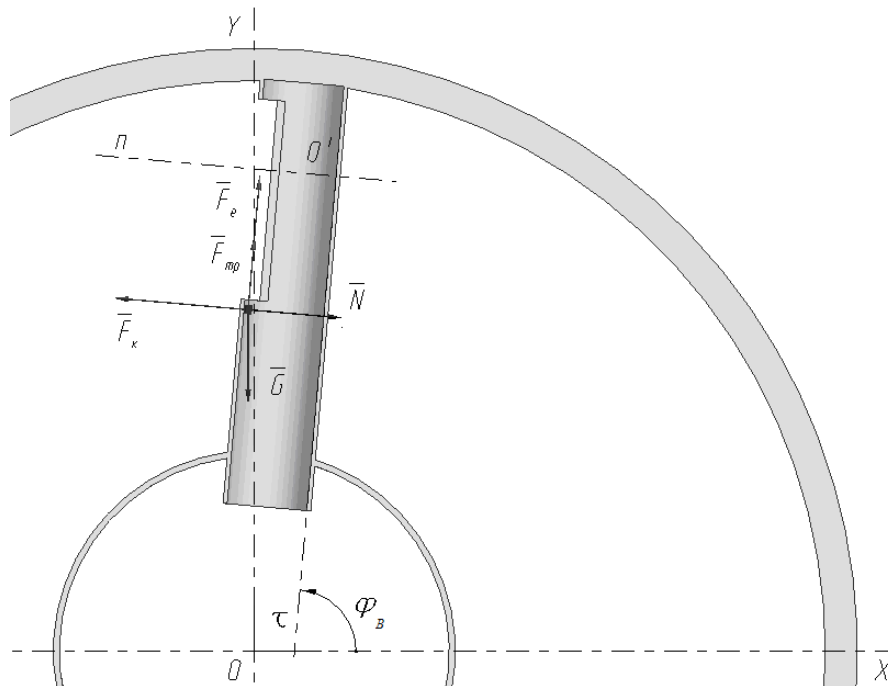


Figure 5. The relative movement of the mass point inside the lifter of the intra-mill device after carry-over

In **Figure 6**, there is a graphic representation of the results, obtained by solving the previously stated differential equations. There are functions, linking the dimensionless relative movement of body $\xi(\varphi)$ to lifter's rotation angle φ for mass points at a distance of 1; 1.1; 1.2; 1.3; 1.4 and 1.5 m.

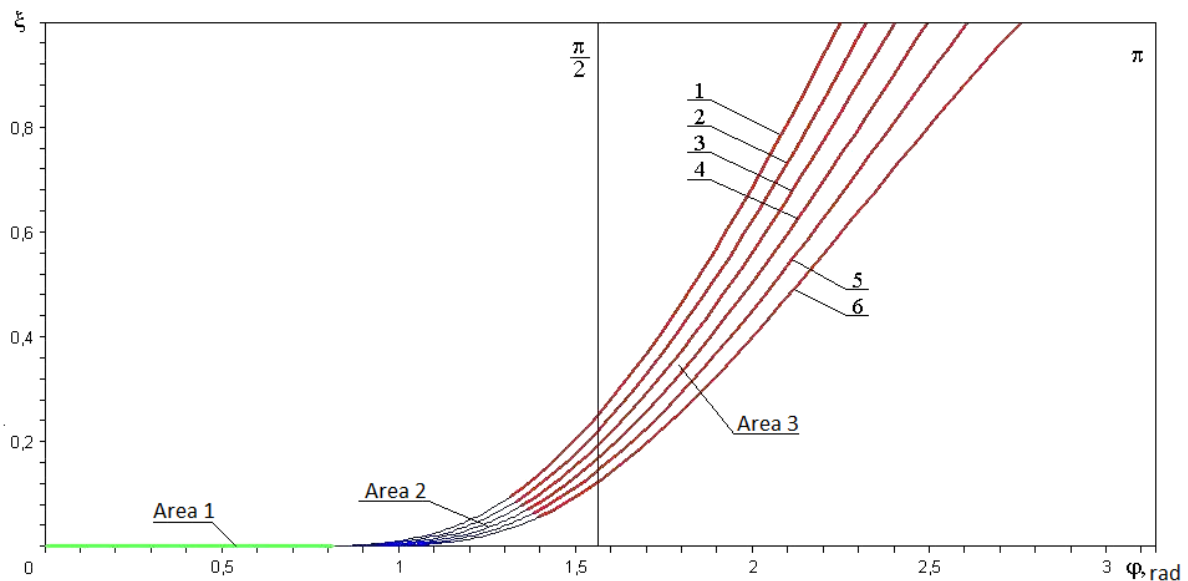


Figure 6. Dependency of dimensionless variable $\xi(\varphi)$, characterizing the relative movement of the body along the surface of the lifter on the lifter's rotation angle for a tubular mill with $\varnothing 3$ m, $f=0.4$, $\omega=1.778$ rad/s, and initial radii of the body's location: 1 – 1 m; 2 – 1.1 m; 3 – 1.2 m; 4 – 1.3 m; 5 – 1.4 m; 6 – 1.5 m.

Figure 7 shows the diagrams, characterizing the relative movement of the mass points along the lifter's surface.

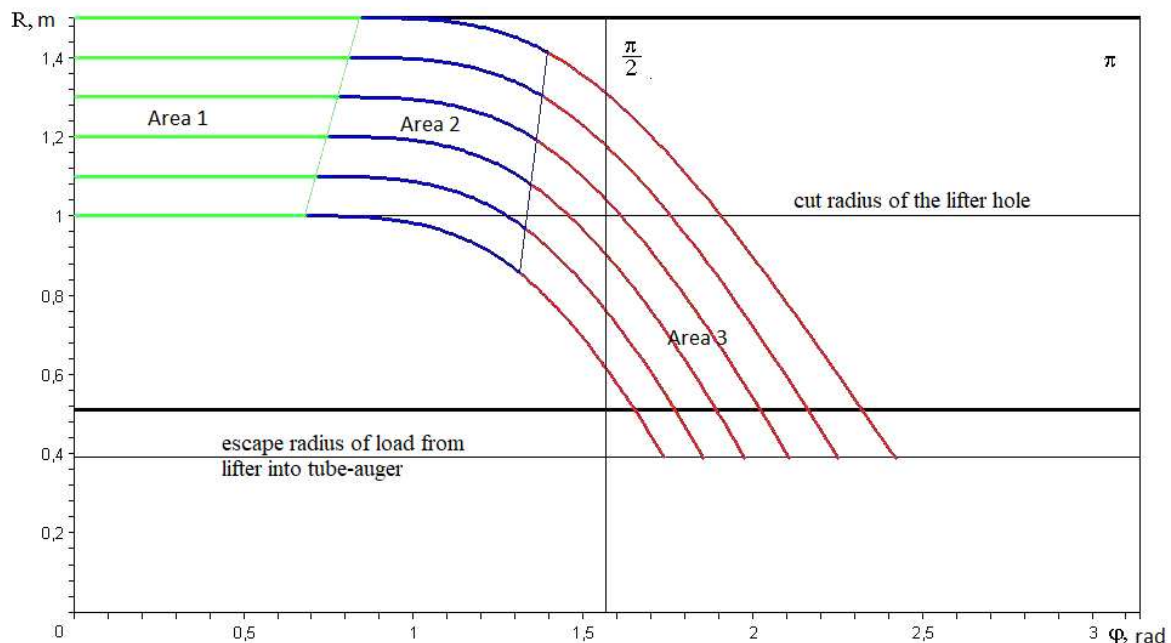


Figure 7. The relative movement of a body along the lifter's surface depending on the lifter's rotation angle for different initial radii of the body's location.

In **Figure 6** and **Figure 7**, the curves in Area 2 reflect solutions of equation (22) satisfying initial conditions (23) for different initial locations, while in Area 3 there are similar curves, corresponding to solutions of equation (25) and initial conditions (26).

Thus, the movement of the load inside the lifter's cavity proceeds in the following way: when the barrel rotates, the grinding bodies and material in the lifter's body are initially motionless with respect to its surface and move with it along the circular trajectories, and at certain rotation angles they start moving along its internal surface in a direction from periphery to the center. Different starting angles α_0 of the relative movement correspond to a different starting position of the load with respect to the axis of rotation. The closer is the layer of the load to the axis of rotation, the sooner it starts participating in the relative motion. Each layer has its corresponding angle α_1 for switching the movement mode. At lifter's rotation angles $\alpha_0 \leq \varphi \leq \alpha_1$ the load is moving following equation (22). During the rotation at the angle of α_1 , a relevant load layer is carried-over from one side of the lifter's surface to the other.

Until this moment, only a part of the load is closer to the axis of rotation than $R-h_{OT}$ (in Figure 6 it is less than $R=1m$), which leads to the load's slinging out.

With the help of the previously described equations for a mass point movement inside the lifter's cavity, one may determine the cut point, dividing the load inside the lifter's cavity into two areas: A and B, with different character of movement.

Figure 8 gives an example of the cut point surface for a mill with a diameter of 3 m, when $f=0.4$ and $\omega=1.778$ rad/s.

If a body is in area A, then, during the movement, it shifts to the free fall trajectory, leaves the lifter cavity and does not end up in the tube-auger's cavity.

If at the breakaway moment the body is in area B, it stays in the lifter's cavity and continues movement along its track.

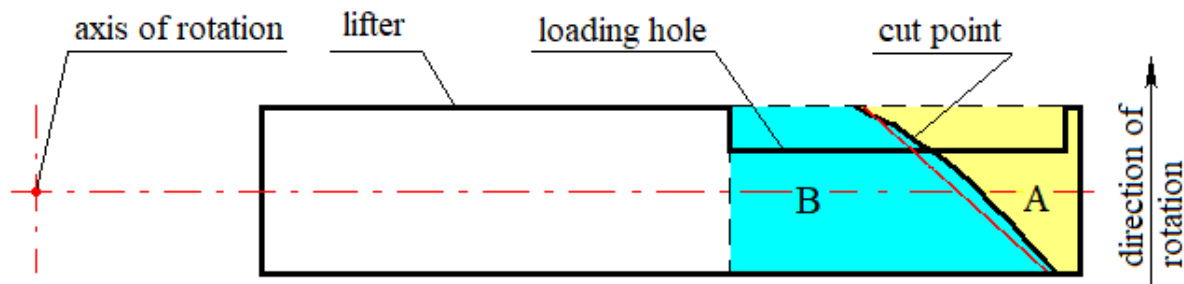


Figure 8. Load cut point in the lifter

3. Conclusion

The mathematical modeling resulted in obtaining analytical and graphic dependencies, allowing determining an initial moment and functions that describe the load's movement with respect to the intra-mill recirculation device lifter's surface.

During the modeling, the moment and conditions were determined, when a carry-over of the load to the opposite wall of the lifter takes place, as well as the functions, describing load's movement at this stage. A cut point was found in the lifter's cavity, allowing determining the part of the load that slings out of the lifter's cavity.

The obtained equations allow designing the intra-mill devices for tubular mills at a totally new level and assessing its influence on the milling process.

4. Acknowledgments

The article was prepared within the development program of the Flagship Regional University on the basis of Belgorod State Technological University named after V.G. Shoukhov, using equipment of High Technology Center at BSTU named after V.G. Shukhov.

References

- [1] Fadin Y M, Latyshev S S, Gavrilenko A V, Arkatova K G and Bogdanov N E 2014 *Journ. of*

- Engin. and Appl. Sc. (ARPN)* **9(11)** 2327-2336
- [2] Bogdanov V S, Fadin Y M, Lozovaya S Y, Latyshev S S, Bogdanov N E and Vasilenko O S 2016 *B IJPT (Hyderabad, India)* **8(3)** 19031-19041
- [3] Bogdanov V S, Mordovskaya O S, Voronov V P, Khanin S I and Kirilov I V 2014 *Journ. of Engin. and Appl. Sc. (ARPN)* **9(11)** 2371-2375
- [4] Bogdanov V S, Hanin S I, Starchenko D N and Sagitov I A 2014 Distinctive features of the relations between grinding equipment and devices inside ball mill body *Journ. of Engin. and Appl. Sc. (ARPN)* **9(11)** 2344-2350
- [5] Bogdanov V S, Fadin Y M, Latyshev S S, Khludeev V I, Gun'ko A I and Nerastenko V Z 2005 *Cement and its application* **1** 49-53
- [6] Bogdanov V S, Fadin Y M, Latyshev S S and oth. 2005 *Pat. 2246355 RF Tubular mill with an intramill grading device. 20.02.2005; Bul. 5*